Materials Today Communications 15 (2018) 55–60

Contents lists available at ScienceDirect

Materials Today Communications

journal homepage: www.elsevier.com/locate/mtcomm

Platinum aptasensor wire arrays for cardiac biomarker detection

Mitali Patil[a,*], Fatima Umanzor[b], Robert Kormos[a,c,d,f], Prashant N. Kumta[a,e,f,**]

[a] Department of Bioengineering, Swanson School of Engineering, University of Pittsburgh, 3700 O'Hara St., Pittsburgh, PA 15261, United States
[b] Department of Chemical and Biomolecular Engineering, John Hopkins University, 3400 N. Charles St., Baltimore, MD 21218, United States
[c] Division of Cardiothoracic Surgery, University of Pittsburgh School of Medicine, 3550 Terrace St., Pittsburgh, PA 15261, United States
[d] Heart and Vascular Institute, University of Pittsburgh Medical Center Presbyterian, 200 Lothrop St., Pittsburgh, PA 15213, United States
[e] Department of Chemical and Petroleum Engineering, Department of Mechanical Engineering and Materials Science, Swanson School of Engineering, University of Pittsburgh, 3700 O'Hara St., Pittsburgh, PA 15261, United States
[f] McGowan Institute of Regenerative Medicine, University of Pittsburgh, 450 Technology Drive, Pittsburgh, PA 15219, United States

ARTICLE INFO

Keywords:
Platinum
Aptasensor
Impedance
Brain-natriuretic peptide
Troponin-T
Cardiovascular disease

ABSTRACT

There is clinical diagnostic power in developing point-of-care diagnostic biosensors offering rapid and sensitive detection of cardiac biomarkers. This could provide outpatient screening and monitoring of cardiovascular diseases in outpatient settings via portable technology. This study focuses on development of platinum wire platforms functionalized with aptamers to impedimetrically detect Brain Natriuretic Peptide (BNP) and Troponin T (TnT), biomarkers, the currently accepted gold standard indicators of congestive heart failure and myocardial infarction. Various platinum wire diameters and surface preparation conditions were selected to determine ideal electrode parameters for impedimetric detection of BNP and TnT without loss of precision and sensitivity. Ideal parameters of 0.5 mm diameter wire polished to 5 μm demonstrated optimal linearity, correlation, and precision when detecting BNP and TnT. The authors have thus developed a simplistic platinum wire multi-array apatasensor platform for detecting BNP and TnT easily expandable to detecting various biomarkers in portable or handheld POC biosensing device configurations.

1. Introduction

There is an increasing demand for sensitive point-of-care (POC) technologies to rapidly monitor the concentrations or activities of biomolecules in biological samples in a cost-efficient manner [1]. Electrochemical impedance spectroscopy (EIS) is ideal for POC biosensors as EIS is a highly sensitive, inexpensive, and label-free technique that is amenable to miniaturization, rendering EIS based biosensors highly promising for direct use at the patient bedside, in-ambulance use by paramedics, or during clinical visits as a useful screening device [2]. However, only electrochemical blood glucose sensors have achieved technological and commercial success despite the need for better and cheaper diagnostics in various other fields and industries, especially in the field of cardiovascular medicine [1]. According to the World Health Organization, cardiovascular diseases (CVDs) are the leading cause of death globally, causing approximately 17.5 million deaths in 2012, accounting for 31.9% of the deaths in the U.S. alone [3]. In addition, CVDs account for 17% of national health expenditures, approximately $273 billion in direct medical costs, and by 0130, 40.5% of the US population is projected to have some form of CVD, causing direct medical costs of CVDs to triple to $818 billion [4]. Therefore, CVDs will remain the leading cause of death in developed countries due to the lack of standard methods of CVD outpatient diagnosis and their silent nature until serious complications arise [5,6]. Therefore, there is a need to develop POC biosensors that can quickly and efficiently diagnose the risk or presence of CVDs in individuals in clinical and emergency settings by precisely and accurately measuring the presence and levels of cardiac biomarkers in blood [6].

Currently, antibodies and enzymes are commonly utilized as detection elements in biosensors due to their high affinity and specificity, but they have relatively short shelf lives. In addition, they are restricted by in vivo parameters, suffer from batch to batch variation, and are highly sensitive to chemical and temperature changes. Therefore, the use of aptamers (oligonucleotides synthesized to bind to their target

Abbreviations: POC, point-of-care; EIS, electrochemical impedance spectroscopy; CVDs, cardiovascular diseases; BNP, brain natriuretic peptide; TnT, troponin T; CHF, congestive heart failure; MI, myocardial infarction; CAD, coronary artery disease; VAPAA, vertically aligned platinum wire-based aptasensor array; PBS, phosphate buffered saline; CPE, constant phase element; R_{ct}, charge-transfer resistance; R_s, solution resistance

* Corresponding author.
** Corresponding author at: 815 E Benedum Hall, Department of Bioengineering, 3700 O'Hara Street, University of Pittsburgh, Pittsburgh, PA 15261, United States.
E-mail addresses: msp47@pitt.edu (M. Patil), pkumta@pitt.edu (P.N. Kumta).

https://doi.org/10.1016/j.mtcomm.2018.02.018
Received 29 January 2018; Accepted 13 February 2018
Available online 21 February 2018
2352-4928/ Published by Elsevier Ltd.

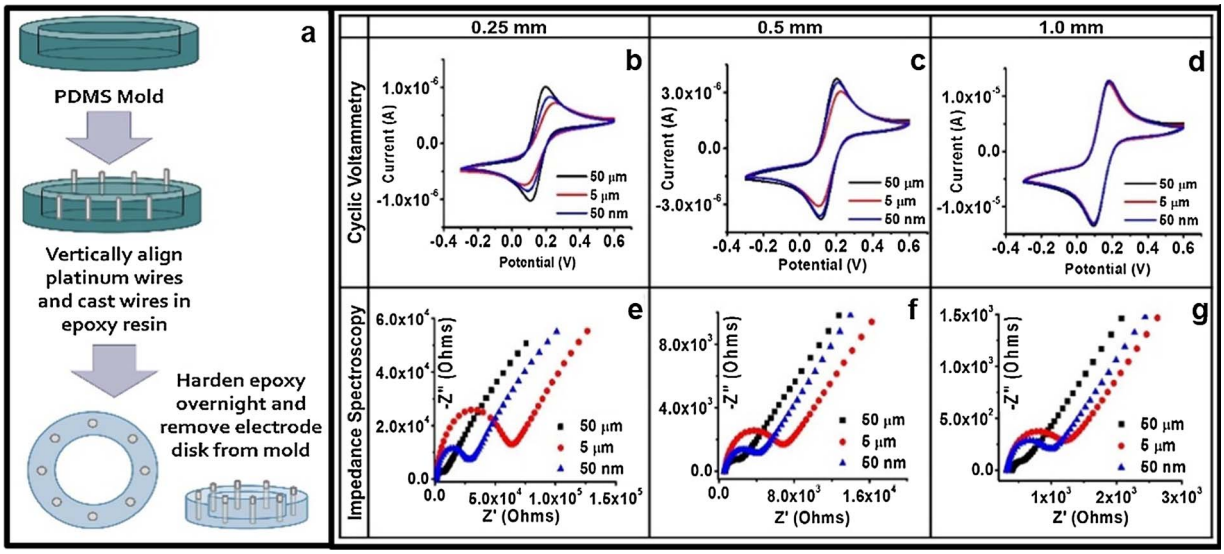

Fig. 1. Layout of platinum electrode disk preparation (a), cyclic voltammagrams at a scan rate of 100 mV/s (b–d), and Nyquist interpretations (e–g) of EIS experiments conducted in 5 mM ($Fe(CN_6)^{3-/4-}$) in 10 mM PBS, with Ag wire as reference electrode and Pt wire counter electrode across 300,000 Hz–0.01 Hz at 10 mV rms AC voltage for platinum electrodes of three polishing grits (50 µm, 5 µm, 50 nm) at different platinum wire diameters – 0.25 mm (b, e), 0.5 mm (c, f), and 1.0 mm (d, g) demonstrating the differences in peak current, peak separation, and impedance between polishing grits at different diameters.

with high affinity and specificity) could considerably improve the biosensor efficiency and sensitivity due to high stability, long shelf lives, and minimal batch-to-batch variations [7]. In addition, there have been few cardiac aptasensors developed, and most of these aptasensors use methods other than EIS to target for biomarkers such as Troponin I, C-Reactive Protein, or Myoglobin individually [8–10]. We plan to target the following two cardiac biomarkers, namely, brain natriuretic peptide (BNP) and Troponin T (TnT) simultaneously on a single device. BNP is a polypeptide secreted by heart ventricles into the bloodstream upon excessive stretching of cardiomyocytes during cardiac stress, thus serving as an indicator for congestive heart failure (CHF) and coronary artery disease (CAD). TnT, on the other hand, is a protein released into the bloodstream upon myocyte injury or death during cardiac injury, thus serving as an indicator for myocardial infarctions (MI) [11–14]. Therefore, tailoring a biosensor to detect these two cardiac markers would be of significant interest to the cardiovascular health community, especially in the detection and monitoring of prominent CVDs such as CHF, CAD, and MI.

To successfully construct an impedimetric biosensor, a conductive material interface biocompatible with the biological detection element is critical. In this context, platinum is an ideal candidate due to its noble metal status, high conductivity, biocompatibility, and low adsorptivity for proteins to adsorb to its surface compared to other noble metals such as gold [15]. This low adsorptivity of proteins to adsorb on platinum surfaces can potentially reduce biofouling and adhesion of target proteins to the surface, thus ensuring that the proteins are only captured by the biological detection element. In addition, platinum, despite being a more inert and less adsorptive noble metal compared to gold, can still serve as an excellent thiolate contact material that has potential for molecular electronic applications such as biosensing [16]. Most biosensor studies conducted on platinum interfaces still utilize antibodies and enzymes as detection elements, and often use platinum electrodes or nanoparticles in tandem with other material interfaces such as carbon nanotubes/nanocomposites [17], graphene [18], chitosan [19], silica [20], polymers [21], or gold [22]. A careful analysis of the literature to date indicates that there are no reported cardiac aptasensor studies conducted that detect multiple cardiac biomarkers exclusively using a platinum interface.

The present study was therefore conducted to report the first account of developing a simplistic vertically aligned platinum wire-based aptasensor array (VAPAA) for the impedimetric detection of cardiac markers, BNP and TnT. Platinum wires of various diameters and surface roughnesses were functionalized to bind BNP and TnT-specific aptamers to the surface and were then tested against various clinically relevant concentrations of BNP and TnT to determine the ideal electrode parameters necessary for fabrication and development of sensitive, precise, and efficient biosensors.

2. Materials & methods

2.1. Reagents

Potassium ferrocyanide and Potassium ferricyanide were purchased from Fisher Scientific, Cysteamine was purchased from Acros Organics, and Glutaraldehyde was purchased from Sigma-Aldrich. Avidin was purchased from Thermo-Fischer Scientific, brain natriuretic peptide (BNP) and TroponinT (TnT) biotinylated aptamers were purchased from OTC Biotech (aptamer sequences are under the protection of OTC Biotech and cannot be disclosed without contacting the company directly). BNP antigen was purchased from ABDSerotec, and TnT antigen was purchased from LeeBio. All the aqueous solutions needed were either prepared in Phosphate-Buffered Saline (PBS) purchased from Lonza or Millipore de-ionized water (18 MΩ cm^{-1}).

2.2. Electrode preparation

Vertically aligned platinum wires (0.25 mm dia, 0.5 mm dia, and 1.0 mm dia, 99.9% metals basis, Alfa-Aesar) were cast in a non-conducting epoxy resin disk (Buehler) in a circular pattern so that 8 platinum electrodes were housed in each disk (Fig. 1a) and polished to 50 µm on 320 grit, 5 µm on 1200 grit, and 50 nm and 2400 grit silicon carbide (SiC) paper (Allied High Tech Products, Inc.). The resulting disk was sonicated in de-ionized water followed by 95% EtOH for five minutes each prior to electrochemical characterization and functionalization. The electrode disk was designed to ensure that each set of electrodes (categorized by diameter) were exposed to the same polishing, characterization, and functionalization techniques and conditions.

2.3. Electrochemical characterization

All the electrochemical characterization was carried out using a

Gamry series G Potentiostat in an electrolyte solution of 5 mM potassium ferro/ferricyanide redox couple in 10 mM PBS ($Fe(CN)_6^{3-/4-}$), utilizing silver wire as the reference electrode and platinum wire as the counter electrode. For electrode characterization, both cylic voltammetry (CV) and electrochemical impedance spectroscopy (EIS) experiments were conducted, and for functionalization and antigen binding assessments, EIS experiments were executed after each step. CV experiments were carried out across a potential range of −0.4 V to 0.6 V at a scan rate of 100 mV/s, and EIS experiments were directed across a frequency range of 300,000 Hz–0.01 Hz with an AC voltage amplitude of 10 mV rms, and were analyzed using the Z-view (Scribner Associates, Inc.) software to determine the specific charge-transfer resistances.

2.4. Electrode functionalization

Platinum electrodes were treated with 10 mg/mL cysteamine prepared in de-ionized water for 1 h at room temperature, followed by 25% glutaraldehyde in water for 1 h at room temperature for thiolation and carboxylation of the surface. The surface was then treated with 1 mg/mL neutravidin prepared in 10 mM PBS for 2 h at room temperature, followed by incubation with biotinylated aptamer for 2 h at room temperature. The electrodes were then stored in PBS at 4 °C.

2.5. Antigen testing

Four concentrations for both BNP and TnT were prepared, each falling within the clinical range representing low to high risk for cardiovascular disease (CVD). BNP-aptamer biosensors were thus successively treated with 0.2 ng/mL, 0.6 ng/mL, 1.0 ng/mL, and 2.0 ng/mL BNP, and correspondingly, TnT-aptamer biosensors were successively treated with 0.005 ng/mL, 0.01 ng/mL, 0.02 ng/mL, and 0.04 ng/mL TnT in order to develop a calibration curve for future biosensor testing. It should be noted that the concentrations selected not only fall within the clinical ranges for BNP (> 0.3 ng/mL is prognostic for unstable heart function, and higher levels, especially near and above 1 ng/mL, typically indicate greater degree of heart failure) and TnT (> 0.01 ng/mL levels of TnT are prognostic for heart attacks), but also go beyond the minimum and maximum limits of the accepted clinical ranges. EIS measurements were then taken after each antigen incubation for obtaining the calibration curves. All the antigen binding steps were conducted at room temperature for 5 min to examine the rapidity of detection by the biosensor.

3. Results & discussion

3.1. Characterization of the electrode parameters

Three disks of vertically aligned platinum wire electrodes were prepared utilizing 0.25 mm diameter (0.059 mm^2 surface area), 0.5 mm diameter (0.19 mm^2 surface area), and 1.0 mm diameter (0.79 mm^2 surface area) platinum wire electrodes. Each disk was polished with each of the three grits (50 µm, 5 µm, 50 nm), thus, creating a total set of nine parameters that were characterized, functionalized, and tested for antigen detection. Electrochemical characterization of the bare platinum electrodes for the nine possible parameters (Fig. 1, Table 1) demonstrate that an increase in wire diameter leads to an increase in current, allowing for more facile passage of current through the electrode (Fig. 1b–d, Table 1) and a decrease in charge-transfer resistance (Fig. 1e–g, Table 1). As the diameter of the electrode increases, the peak currents tend to cluster together, demonstrating that polishing has less impact on the current passage with greater surface area. In addition, within a given diameter (i.e. within 0.25 mm), the polishing differences are less pronounced than between the different diameters (i. e. between 0.25 mm and 1.0 mm), thus demonstrating that while polishing introduces minor differences, the change in diameter introduces the more dramatic difference observed in peak currents and impedance. The electrode polished with 50 µm polishing medium always exhibits the highest peak currents (due to higher surface area), while 5 µm inevitably exhibits the lowest peak currents. These trends are also observed in the Nyquist interpretations of EIS experiments, with 50 µm polished electrodes displaying the lowest charge-transfer resistance while 5 µm polished electrodes display the highest charge-transfer resistance. While the range of charge-transfer resistances across polishing do decrease, there are still substantial differences between the polishing grit sizes, especially between 50 µm and 5 µm, thus establishing EIS as a highly sensitive technique compared to the exclusively current based experiments such as cyclic voltammetry.

Table 1
Numerical values corresponding to Fig. 1 depicting peak cathodic currents and peak anodic currents for cyclic voltammagrams and charge-transfer resistance for Nyquist plots derived from electrochemical impedance spectroscopy between different polishing grits at different diameters.

Pt Dia.	Particle Size	Cyclic Voltammetry		Impedance Spectroscopy R_{ct} (Ω)
		I_{pC} (µA)	I_{pA} (µA)	
0.25 mm	50 µm	1.223	−1.203	4558
	5 µm	0.829	−0.829	57053
	50 nm	1.005	−0.973	24568
0.5 mm	50 µm	4.248	−4.260	1205
	5 µm	3.495	−3.463	5352
	50 nm	4.005	−4.027	3030
1.0 mm	50 µm	15.62	−15.84	158.3
	5 µm	15.20	−15.46	747.5
	50 nm	15.33	−15.57	568.3

3.2. Biosensor functionalization and antigen detection

All the charge-transfer resistances obtained from EIS characterization for all the nine parameters of the biosensors at any stage of the experiment fit the equivalent circuit shown in Fig. 2a, which depicted a solution resistance (Rs, due to the ferro/ferricyanide electrolyte couple) in series with the two constant phase element (CPE) components, with each CPE component in parallel to a resistance (Rct) component. The CPE components result from an electrochemical double layer, which is indicative of exposure of the electrode to the electrolyte, thus creating two parallel layers of charge – the first layer being the surface charge resulting from the surface chemical interactions, while the second layer constitutes the ions attracted to but loosely associated with the surface charge (known as a diffuse layer). Each CPE-R_{ct} circuit was marked as inner layer or outer layer, with the inner layer being the semicircular portion of the Nyquist plot, and the outer layer being the second portion of the Nyquist plot, which would represent a second semicircle with further extrapolation. The inner layer represented the chemical interaction of interest, while the outer layer represented the possible interaction of ions with other charged layers of the electrode/biosensor. Fig. 2b and c demonstrates the multiple chemical interactions required to bind the detection element (aptamers) to the platinum electrode surface for the representative electrode made from 0.5 mm diameter Pt wire polished using 5 micron polishing SiC grit. Cysteamine, glutaraldehyde, Avidin, and aptamer were added in succession to one another, followed by storage in PBS (which served as the buffer fluid and as the 0.00 ng/mL baseline for antigen detection experiments). As each component was sequentially added to the biosensing surface, the charge transfer resistance increased (Fig. 2b, Table S1), with Avidin binding demonstrating the largest change in charge-transfer resistance with respect to the previous functionalization step due to its large size compared to cysteamine, glutaraldehyde, and aptamers. Once the biosensors were prepared, the biosensors were tested for antigen detection for four clinically relevant concentrations of BNP (Fig. 2d, Table S2) and TnT (Fig. 2e, Table S2), respectively. As the antigen concentration

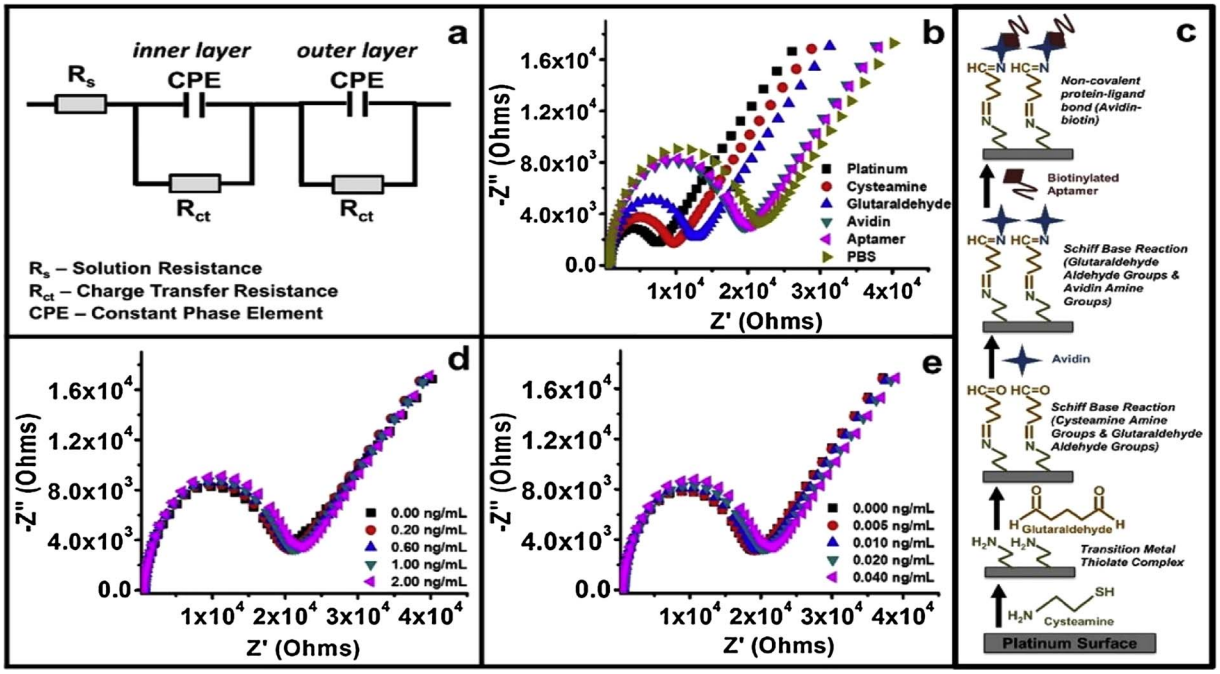

Fig. 2. (a) Equivalent circuit used for fitting and determination of charge-transfer resistance values in following Nyquist plots, (b) Nyquist interpretation of EIS experiments conducted after each step of functionalization for the biosensor (10 mg/mL cysteamine, 25% glutaraldehyde, 1 mg/mL Neutravidin, and 150 μg/mL aptamer), (c) Functionalization schematic with accompanying chemical interactions between functionalization layers (d) Nyquist interpretation of EIS experiments conducted after each successive concentration of BNP demonstrating an increase in charge-transfer resistance with an increase in BNP concentration, (e) Nyquist interpretation of EIS experiments conducted after each successive concentration of TnT demonstrating an increase in charge-transfer resistance with an increase in TnT concentration. All EIS experiments were conducted in 5 mM $(Fe(CN_6)^{3-/4-})$ in 10 mM PBS, with 5 μm polished 0.5 mm diameter platinum working electrodes, Ag wire reference electrode, and Pt wire counter electrode across 300,000 Hz–0.01 Hz at 10 mV rms AC voltage.

increased, the charge transfer resistance increased, thus indicating that as more antigen was bound to the aptamer-functionalized biosensors, the impedance correspondingly increased. These successive increases in impedance allow for the concentration to be electrochemically quantified as a specific charge-transfer resistance value.

3.3. Linearity and reproducibility of calibration curves for biosensor parameters

Once all the nine parameters were electrochemically tested for both BNP and TnT antigen detection through EIS, the percent change between each antigen charge-transfer resistance value and the baseline charge-transfer resistance value obtained for PBS was calculated and plotted against the concentration to determine the calibration curve for each parameter for both BNP (Fig. 3a–c, Table 2) and TnT (Fig. 3d–f, Table 2). Saturation of these clinically relevant levels is indicative of low sensitivity of the biosensor at these crucial concentrations. However, the linearity is indicative of the success of the biosensor to detect within the crucial concentration range and possibly beyond that range as well. Standard error (n = 3) was calculated for each concentration and for each parameter, with a smaller standard error reflective of precision and reproducibility while the larger standard errors serving as an indicator of inconsistency across the electrodes. Therefore, the parameter that demonstrated excellent linearity and precision for both BNP and TnT would be considered the ideal parameters for all future experimentation. At 0.25 mm diameter, all but one parameter (50 nm) saturates for BNP (Fig. 3a), and all parameters saturate for TnT (Fig. 3d). On the other hand, for 0.5 mm diameter Pt wire, both 50 μm and 5 μm for BNP demonstrate linearity, but the correlation between concentration and percent change in charge-transfer resistance is smaller for 50 μm ($R^2 = 0.89$) than for 5 μm ($R^2 = 0.98$). All the parameters save for 5 μm saturated in TnT (Fig. 3e), and the 5 μm calibration curve had an excellent correlation ($R^2 = 0.98$). However, for 1.0 mm diameter Pt wire, all the polishing parameters saturate for both BNP (Fig. 3c) and TnT (Fig. 3f). Another minor aspect to note is that for the 0.25 mm wire, 5 μm and 1.0 mm wire, 50 nm, we see that the calibration curve dips below 0% change R_{ct}. This drop at the beginning of the calibration curve could be the result of instability of the functionalization layers for those particular parameters, perhaps either due to smoothness of the surface (50 nm polish) or the small area (0.25 mm diameter), although human error may also contribute to possible damage or improper binding of the layers. Therefore, the ideal parameter was determined to be 0.5 mm diameter wire polished to 5 μm. This parameter may have been ideal due to the fact that the rougher surfaces (50 μm) tend to be better for protein attachment than the polished and more smoother surfaces (50 nm) due to the presence of a greater surface area, but rougher surfaces can also induce greater protein denaturation [23,24]. Hence, a surface that is between these two spectra would be considered ideal (5 μm). The same compromise could be extended to interpretation of the results for the wire diameters, wherein the smaller diameter (0.25 mm) had reduced area for binding, while the larger diameter (1.0 mm) had larger area for binding, but also a higher probability of expressing inconsistences or defects on the surface [25,26], justifying the middle diameter (0.5 mm) to be the ideal condition.

4. Conclusions

In summary, we have designed a simplistic upright vertically aligned platinum wire-based aptasensor multi-array (VAPAA) impedimetric biosensor that can detect markers indicative of myocyte stress (BNP) and myocyte injury (TnT). This design is label-free (i.e. no fluorescent tagging) and is more cost-effective. Furthermore, once scaled down and miniaturized, the integration would avoid expensive instrumentation. We also determined the ideal parameters (0.5 mm platinum wire polished to 5 μm) necessary for further experimentation. Therefore, future experimentation would extend to detection of other cardiac markers followed by miniaturization of the potentiostat circuitry and repetitive testing to ensure accuracy, precision, selectivity, and sensitivity. Future experiments will also especially focus on

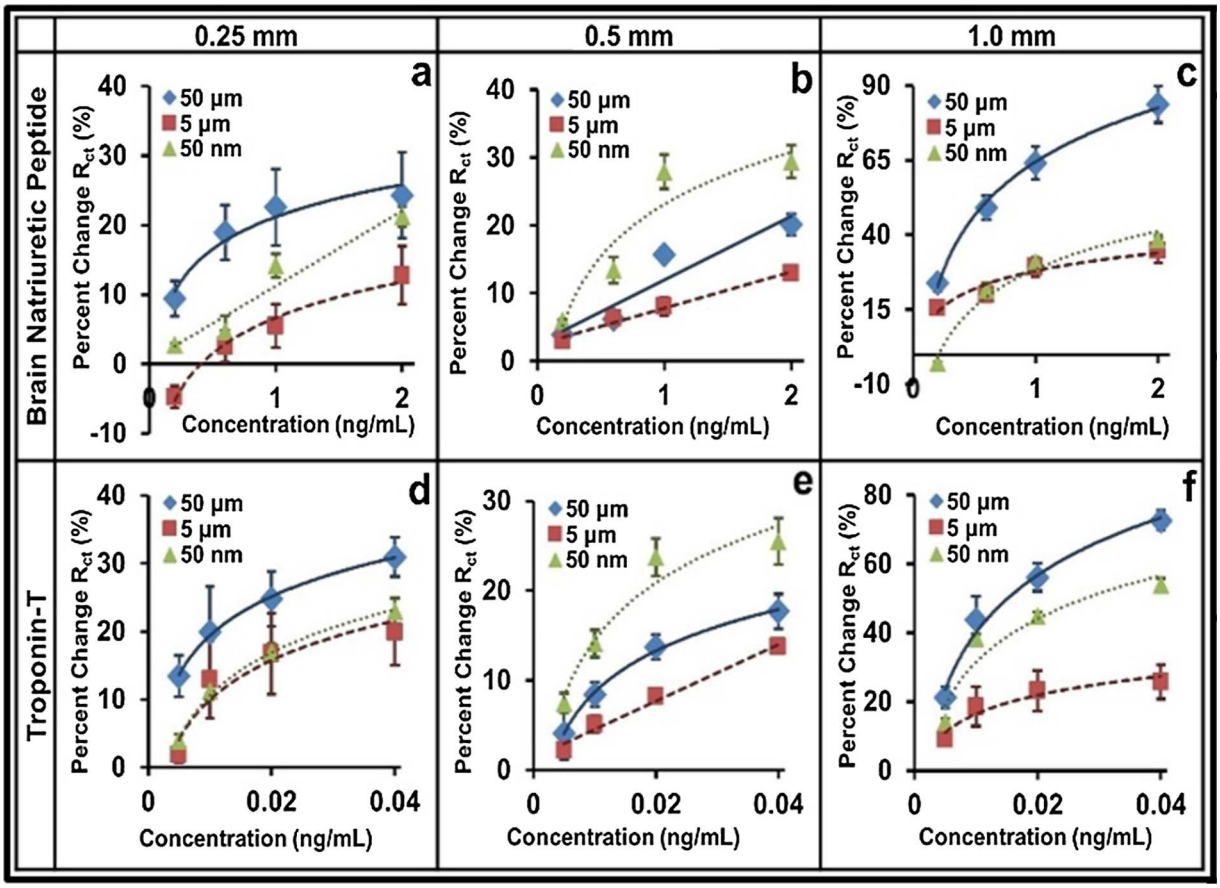

Fig. 3. Calibration curves depicting average percent change in charge-transfer resistance as a function of concentration and standard error (n = 3) for aptasensors utilizing three polishing grits (50 µm, 5 µm, 50 nm) for different platinum wire diameters – 0.25 mm (a, d), 0.5 mm (b, e), and 1.0 mm (c, f) for both BNP concentrations 0.25 ng/mL, 0.5 ng/mL, 1.0 ng/mL and 2.0 ng/mL (a–c), and TnT concentrations of 0.005 ng/mL, 0.01 ng/mL, 0.02 ng/mL, and 0.04 ng/mL (d–f).

Table 2
Corresponding calibration curve equations and correlations for each diameter and polishing grit corresponding to the increase in charge-transfer resistance with successive concentrations of BNP and TnT.

Pt Dia.	Particle Size	Brain Natriuretic Peptide (BNP)	Troponin T (TnT)
0.25 mm	50 µm	y = 6.69ln(x) + 21.20 R^2 = 0.95	y = 8.28ln(x) + 57.55 R^2 = 1.00
	5 µm	y = 7.43ln(x) + 6.69 R^2 = 0.98	y = 8.40ln(x) + 48.60 R^2 = 0.90
	50 nm	y = 10.79ln(x) + 0.49 R^2 = 0.94	y = 9.20ln(x) + 52.52 R^2 = 1.00
0.5 mm	50 µm	y = 9.39x + 2.59 R^2 = 0.89	y = 6.65ln(x) + 39.31 R^2 = 1.00
	5 µm	y = 5.35x + 2.51 R^2 = 0.98	y = 315.92x + 1.40 R^2 = 0.98
	50 nm	y = 11.09ln(x) + 23.13 R^2 = 0.89	y = 9.19ln(x) + 56.83 R^2 = 0.94
1.0 mm	50 µm	y = 26.00ln(x) + 64.46 R^2 = 1.00	y = 24.05ln(x) + 150.86 R^2 = 0.99
	5 µm	y = 8.60ln(x) + 27.98 R^2 = 0.92	y = 7.87ln(x) + 52.67 R^2 = 0.93
	50 nm	y = 18.29ln(x) + 28.55 R^2 = 0.98	y = 18.14ln(x) + 115.04 R^2 = 0.91

improving the sensitivity of the ideal parameter determined from this paper, as a more pronounced change in charge-transfer resistance between the different concentrations would enhance the performance of the biosensor and its ability to distinguish between the different concentrations of target biomarkers. Therefore, future experiments will focus on further optimizing the parameters on the 0.5 mm diameter, 1200 grit (5 µm) polished Pt surface described herein, especially the functional layer concentrations, incubation times, and whether certain functional layers can be removed without impacting the biosensor effectiveness (which will reduce the complexity and thus also reduce the potential for error). Future experiments will also mandate the use of clinically relevant samples to ensure that the biosensors can function in biological samples, especially to address the possible interference that biological samples can cause to the non-detecting layers (layers aside from the aptamer). Together, this would enable successful antigen detection in whole blood samples and possibly other bodily fluids, potentially fulfilling the end goal of developing a selective and sensitive cardiac biomarker sensor. Once the biosensing platform is fully optimized and established with both laboratory prepared samples and clinically/biologically derived samples, then the nature of the platinum material interface can be changed. Rather than being limited to vertically aligned mm diameter wires, the platinum interface can also be potentially restructured as nanoparticles [27] or nanowires [27], or potentially even thin films [28], which might be more amenable with microfludics and interdigitated circuits for biosensor miniaturization. With the follow-on planned integration, the technology can be translated into a handheld sensor device for rapid detection of the additional biomarkers. In addition, this technology can be extended to antibodies and enzymes, not just aptamers, allowing the range of biological detection elements and detectable antigens to be widespread, therefore serving as a universal biosensing platform.

Acknowledgements

The authors acknowledge partial financial assistance of NSF-ERC Grant #EEC-0812348 in supporting this work. The authors also

acknowledge financial support of Swanson School of Engineering, University of Pittsburgh, while P.N. Kumta acknowledges the Edward R. Weidlein Chair Professorship, Center for Complex Engineered Multifunctional Materials (CCEMM), and NSF-CBET Grant #0933153 for support of use of equipment and accessories.

Appendix A. Supplementary data

Supplementary data associated with this article can be found, in the online version, at https://doi.org/10.1016/j.mtcomm.2018.02.018.

References

[1] Z. Guo, L. Murphy, V. Stein, W.A. Johnston, S. Alcala-Perez, K. Alexandrov, Engineered PQQ-Glucose dehydrogenase as a universal biosensor platform, J. Am. Chem. Soc. 138 (2016) 10108–10111.
[2] I.O. K'Owino, O.A. Sadik, Impedance spectroscopy: a powerful tool for rapid biomolecular screening and cell culture monitoring, Electroanalysis 17 (23) (2005) 2101–2113.
[3] A.S. Go, et al., Heart disease and stroke statistics − 2014 update: a report from the American Heart Association, Circulation 129 (2014) 282–292.
[4] P.A. Heidenreich, et al., Forecasting the future of cardiovascular disease in the United States: a policy statement from the American Heart Association, Circulation 123 (2011) 933–944.
[5] R.E. Gerszten, T. Wang, J.;*1*; The search for new cardiovascular biomarkers, Nature 451 (2008) 949–952.
[6] W.B. Gibler, A.L. Blomkalns, Point-of-care testing for cardiac biomarkers in the ED: A blueprint for implementation, EMCREG Int. 1 (2006) 1–10.
[7] S.D. Jayasena, Aptamers: an emerging class of molecules that rival antibodies in diagnostics, Clin. Chem. 45 (9) (1999) 1628–1650.
[8] H. Jo, H. Gu, W. Jeon, H. Young, J. Her, S.K. Kim, J. Lee, J.H. Shin, C. Ban, Electrochemical aptasensor of cardiac troponin i for the early diagnosis of acute myocardial infarction, Anal. Chem. 87 (19) (2015) 9869–9875.
[9] S.A. Vance, M.G. Sandros, Zeptomole detection of C-reactive protein in serum by a nanoparticle amplified surface plasmon resonance imaging aptasensor, Sci. Rep. 4 (2014) 5129.
[10] V. Kumar, M. Shorie, A.K. Ganguli, P. Sabherwal, Graphene-CNT nanohybrid aptasensor for label free detection of cardiac biomarker myoglobin.*Biosens*, Bioelectron 72 (2015) 56–60.
[11] E. Braunwald, Biomarkers in heart failure, New Engl. J. Med. 358 (20) (2008) 2148–2159.
[12] A.S. Jaffe, L. Babuin, F.S. Apple, Biomarkers in acute cardiac disease, J. Am. Coll. Cardiol 48 (1) (2006) 1–11.
[13] R.S. Vasan, Biomarkers of cardiovascular disease, Circulation 113 (2006) 2335–2362.
[14] L. Babuin, A.S. Jaffe, Troponin: the biomarker of choice for the detection of cardiac injury, Can. Med. Assoc. J. 173 (10) (2005) 1191–1202.
[15] X. Jiang, Y. Wu, X. Mao, X. Cui, L. Zhu, Amperometric glucose biosensor based on integration of glucose oxidase with platinum nanoparticles/ordered mesoporous carbon nanocomposite, Sens. Actuators B 153 (2011) 158–163.
[16] D.Y. Petrovykh, H. Kimura-Suda, A. Opdahl, L.J. Richter, M.J. Tarlov, L.J. Whitman, Alkanethiols on platinum: multicomponent self-assembled monolayers, Langmuir 22 (2006) 2578–2587.
[17] A. Siriviriyanun, T. Imae, N. Nagatani, Electrochemical biosensors for biocontaminant detection consisting of carbon nanotubes, platinum nanoparticles, dendrimers, and enzymes, Anal. Biochem. 443 (2013) 169–171.
[18] P. Kannan, T. Maiyalagan, N.G. Sahoo, M. Opallo, J. Nitrogen doped graphene nanosheet supported platinum nanoparticles as high performance electrochemical homocysteine biosensors, Mater. Chem. B 1 (2013) 4655–4666.
[19] A. Safavi, F. Farjami, Electrochemical biosensors for biocontaminant detection consisting of carbon nanotubes, platinum nanoparticles, dendrimers, and enzymes, Biosens. Bioelectron. 26 (2011) 2547–2552.
[20] H. Li, J. He, Y. Zhao, D. Wu, Y. Cai, Q. Wei, M. Yang, Immobilization of glucose oxidase and platinum on mesoporous silica nanoparticles for the fabrication of glucose biosensor, Electrochim. Acta 56 (2011) 2960–2965.
[21] V.C. Ferreira, A.I. Melato, A.F. Silva, L.M. Abrantes, Conducting polymers with attached platinum nanoparticles towards the development of DNA biosensors, Electrochem. Commun. 13 (2011) 993–996.
[22] D. Bagal-Kestwal, R.M. Kestwal, B.C. Hsieh, R.L.C. Chen, T.J. Cheng, B.H. Chiang, Electrochemical beta(1–3)-D-glucan biosensors fabricated by immobilization of enzymes with gold nanoparticles on platinum electrode, Biosens. Bioelectron. 26 (2010) 118–125.
[23] A. Dolatshahi-Pirouz, K. Rechendorff, M.B. Hovgaard, M. Foss, J. Chavallier, F. Besenbacher, Bovine serum albumin adsorption on nano-rough plainum surfaces studied by QCM-D, Colloids Surf. B 66 (2008) 53–59.
[24] K. Rechendorff, M.B. Hovgaard, M. Foss, V.P. Zhdanov, F. Besenbacher, Enhancement of protein adsorption induced by surface roughness, Langmuir 22 (2006) 10885–10888.
[25] R. Van Noort, Introduction to Dental Materials, 4th ed., Mosby, 2013 264.
[26] S. Nishida, Failure Analysis in Engineering Applications, 1st ed., Butterworth-Heinemann, 1992 228.
[27] C. Zhu, G. Yang, H. Li, D. Du, Y. Lin, Electrochemical sensors and biosensors based on nanomaterials and nanostructures, Anal. Chem. 87 (1) (2016) 230–249.
[28] V. Torrisi, F. Ruffino, A. Liscio, M.G. Grimaldi, G. Marletta, Emerging interface dipole versus screening effect in copolymer/metal nano-layered systems, Appl. Surf. Sci. 359 (2015) 637–642.